Atorvastatin prolongs the lifespan of radiation-induced reactive oxygen species in PC-3 prostate cancer cells to enhance the cell killing effect

HAO YU, SHAO-QIAN SUN, XIAO-BIN GU, WEN WANG and XIAN-SHU GAO

Department of Radiation Oncology, Peking University First Hospital, Peking University, Beijing 100034, P.R. China

Abstract. Studies have reported that atorvastatin (ATO) may increase the radiosensitivity of malignant cells. However, the influence of ATO on reactive oxygen species (ROS) levels before and after irradiation has not been fully illustrated. In the present study, radiosensitivity was evaluated by a clonogenic assay and a cell survival curve and cell apoptosis was measured by flow cytometry. ROS were detected by a laser scanning confocal microscope and flow cytometry with a DCFH-DA probe. NADPH oxidases (NOXs) and superoxide dismutase (SOD) proteins were detected by immunoblotting, and total SOD activity was measured using an SOD kit. We also conducted transient transfection of *NOX2* and *NOX4* genes to increase intracellular ROS generation and applied SOD mimetic tempol to enhance ROS elimination ability. Our results demonstrated that, with ATO-alone treatment, the survival fractions of irradiated PC-3 cells were significantly decreased. Meanwhile, the apoptosis rate of the irradiated cells increased significantly (P<0.05). The ROS levels of the study group decreased obviously before irradiation (P<0.01), however, the radiation-induced ROS of the study group was at a high level even when irradiation had been terminated for 2 h (P<0.01). Moreover, NOX2 and NOX4 levels and total SOD activity decreased (P<0.01), while the levels of SOD1 were stably maintained (P>0.05). On the other hand, the decreased survival fractions and high radiation-induced ROS levels were abrogated by increasing the level of NOXs by gene transfection or by enhancing the ability of SOD utilizing the addition of tempol. In conclusion, ATO enhanced the cell killing effect of irradiation by reducing endogenous ROS levels and prolonging the lifespan of radiation-induced ROS via a decrease in the level of NOXs and SOD activity.

Introduction

Radiotherapy is one of the main treatments used to deal with malignancy. More than 50% of patients with malignant tumors receive radiotherapy during their treatment (1). Radiation-induced DNA damage is one of main mechanisms underlying the cell killing effect of radiotherapy. Compared with the direct killing effect of irradiation, the indirect killing effect that results from reactive oxygen species (ROS) plays a pivotal role in DNA damage (2). When high-energy rays act on tumor cells, a booming growth of ROS levels occurs in the cytoplasm, then combines with DNA bases and sugar backbones to cause DNA chain fractures. These fractures, if not repaired in time, trigger the process of apoptosis of the cells and ultimately cell death (3).

Statin is a type of 3-hydroxy-3-methyl-glutaryl-CoA (HMGCoA) reductase inhibitor which has been used to lower plasma cholesterol in clinical practice (4). Recently, studies have discovered that statins have the potential to increase the radiation-mediated killing of malignant cells. Park *et al* reviewed 6 studies and concluded that statins have a potential benefit to prostate cancer patients who receive radiotherapy (5). He *et al* found that atorvastatin (ATO) may increase the radiation-mediated killing of PC-3 cells (6). Fritz *et al* found that lovastatin increased the cell killing effect of irradiation in a variety of tumors (7). Moreover, several studies have also reported that statins can influence the intracellular ROS level in tumor cells. Mihăilă found that simvastatin can increase the ROS level in lymphoblasts (8), but Song *et al* reported that lovastatin may inhibit the ROS generation in B-cell lymphoma (9). However, the effects of statins on radiation-induced ROS levels in malignant cells have rarely been investigated.

ATO is a third generation statin. Studies have reported that ATO can influence ROS generation in vascular cells (10). The PC-3 cell line is a typical castrate-resistant prostate cancer (CRPC) cell line which has poor radiosensitivity and strongly resists the cell killing effect of irradiation (11). In the present study, we hypothesized that ATO may also interfere with the ROS generation in PC-3 cells, thereby influencing the

Correspondence to: Professor Xian-Shu Gao, Department of Radiation Oncology, Peking University First Hospital, Peking University, 7 Xishiku Street, Beijing 100034, P.R. China
E-mail: dryh2013@163.com

radiation-induced ROS levels and the cell killing effect. Thus, the clonogenic ability, apoptosis rate, intracellular ROS level and levels of regulatory proteins, such as NOX2, NOX4 and SOD1, were evaluated.

Materials and methods

Reagents. ATO was purchased from Cayman Chemical Co. (Ann Arbor, MI, USA). Tempol was purchased from Enzo Life Sciences, Inc. (Farmingdale, NY, USA) and an apoptosis detection kit was purchased from BD Biosciences (Franklin Lakes, NJ, USA). An ROS assay kit and a SOD assay kit were purchased from Beyotime Institute of Biotechnology (Shanghai, China). Hoechst 33342 staining solution was purchased from Bridgen Company (Beijing, China). A rabbit monoclonal anti-NOX2 antibody and a rabbit monoclonal anti-SOD1 antibody were purchased from Biosynthesis Biotechnology Corp. (Beijing, China) and a rabbit monoclonal anti-NOX4 antibody was obtained from Abcam (Cambridge, UK).

Cell culture. The PC-3 cell line was purchased from the American Type Culture Collection (ATCC, Manassas, VA, USA) and the cells were maintained in RPMI-1640 medium that was supplemented with 10% (v/v) fetal bovine serum (FBS) and cultured at 37˚C in an incubator with 5% CO_2 and a humid atmosphere.

Experimental schedule. To evaluate the radiosensitization potential of ATO on PC-3 cells, clonogenic and apoptosis assays were first conducted. Next, we transiently transfected *NOX2* and *NOX4* genes into the PC-3 cells so that by increasing the expression level of NOXs in the cells and with the addition of tempol, an SOD mimetic, into the cell culture medium, the ROS scavenging ability of the PC-3 cells was increased. In the following experiments, the cells were divided into four groups: vehicle, ATO alone, ATO plus tempol and ATO plus transfected *NOXs*. These grouped cells were applied to an ROS detection assay, an immunoblotting assay and SOD activity detection. Finally, we explored the change in the survival fraction of the PC-3 cells with the clonogenic assay by combining ATO with tempol or by the transfected *NOXs*. All the cells from the study groups were treated with 10 μM ATO for 24 h and the cells with the addition of tempol were treated with 3 mM tempol for another 10 h. Dimethyl sulfoxide (DMSO) was applied to the vehicle as a negative control.

Clonogenic assay. Cells were seeded into seven 6-well plates at different quantities and cultured at 37˚C in an incubator for >24 h. After being pretreated with the vehicle, ATO, tempol or transfected *NOXs*, the medium was renewed and the cells were irradiated with different doses (0, 0.5, 1, 2, 4, 6 and 8 Gy) by a 6 MV X-ray linear accelerator (4 Gy/min at room temperature). Subsequently, the cells were cultured at 37˚C in an incubator for 14 days. When the clusters were >50 cells, colonies were fixed with methanol and stained using methylene blue for cell counting.

A cell survival curve was plotted by GraphPad Prism 6 software according to survival fractions and was calculated as the clonogenic efficiency of the irradiated cells divided by that of the unirradiated cells. The clonogenic efficiency was

calculated as the percentage of the clones of the treated cells divided by that of the control. To calculate the radiosensitivity parameters, including D_0, D_q, N, SF_2 and SERs (12), a cell survival curve was fitted by the multi-target single hit equation: $SF = 1 - (1 - e^{-D/D_0})^N$ (13).

Apoptosis assay. After ATO treatment, the cells from the study group received a 1 Gy dose of irradiation using an Elekta linear accelerator (4 Gy/min at room temperature). Six hours later, all the cells were collected into a 15 ml centrifuge tube, digested with 0.25% trypsin (without 0.05% EDTA) and rinsed thrice with ice-cold phosphate-buffered saline (PBS). Subsequently, the cells were resuspended with 1X Annexin-binding buffer, and then $1x10^5$ cells were transferred into a 1.5 ml Eppendorf tube and 5 μl Annexin-V FITC and 5 μl propidium iodide were added. After 15 min of lucifugal incubation at room temperature, cell apoptosis was detected by flow cytometry. The apoptosis rate was calculated as the early apoptosis rate plus the late apoptosis rate.

RNA extraction and DNA amplification. Total RNA was extracted by TRIzol method according to the manufacturer's instructions (Invitrogen, Carlsbad, CA, USA), c-DNA was synthesized by Reverse transcription PCR kit (Tiangen Biotech Co., Ltd. (Beijing, China). *NOX2* and *NOX4* cDNA were then amplified by a PCR kit (Sangon, Biotech Co., Ltd., Shanghai, China). The *NOX2* primer sequences (sense primer, 5'-TCACTGGAGTTGTCATCACGCTGT-3' and antisense primer, 5'-AAGGGCCCATCAACCGCTATCTTA-3') and the *NOX4* primer sequences (sense primer, 5'-AGCAGA GCCTCAGCATCTGTTCTT-3' and antisense primer, 5'-AGC TTGGAATCTGGGCTCTTCCAT-3') are referred to in published data (14). Briefly, the PCR reaction system was composed of diluted *NOXs* cDNA, 0.1 mM dNTP, 0.2 U/μl *Taq* polymerase, 0.4 pmol/μl of each primer, PCR buffer and deionized water. The procedure steps were as follows: the first step was at 95˚C for 5 min, then the second step to the fourth step were run for 30 cycles at 95˚C for 30 sec, 55˚C for 30 sec and 72˚C for 30 sec and the fifth step was conducted at 72˚C for 7 min.

Recombinant plasmid construction. The amplified DNA was transfected into DH5α competent cells (GenStar, Biosolutions Co., Ltd., Beijing, China) and the plasmid was extracted using a plasmid extraction kit (Life Technologies, Grand Island, NY, USA). The plasmid and pcDNA3.1 vector (Invitrogen) were digested by the restriction enzymes *Bam*HI and *Hin*dIII. Next, *NOX* genes and pcDNA3.1 DNA were purified by agarose gel electrophoresis and extracted by DNA gel extraction kit (ATOM, China) and then the *NOX* genes and the vector were linked by T4 DNA ligase. Finally, the recombinant vector was transfected into DH5α cells again and plasmid extraction was conducted and identified by enzyme digestion, electrophoresis and sequencing.

Transient transfection. Before transfection, the PC-3 cells were seeded into 6-well plates at $2x10^5$ cells/well and cultured in a 37˚C incubator for 48 h. DNA and Lipo3000 transfection reagent (Invitrogen) were diluted using non-serum RPMI-1640 medium, mixed and maintained at room
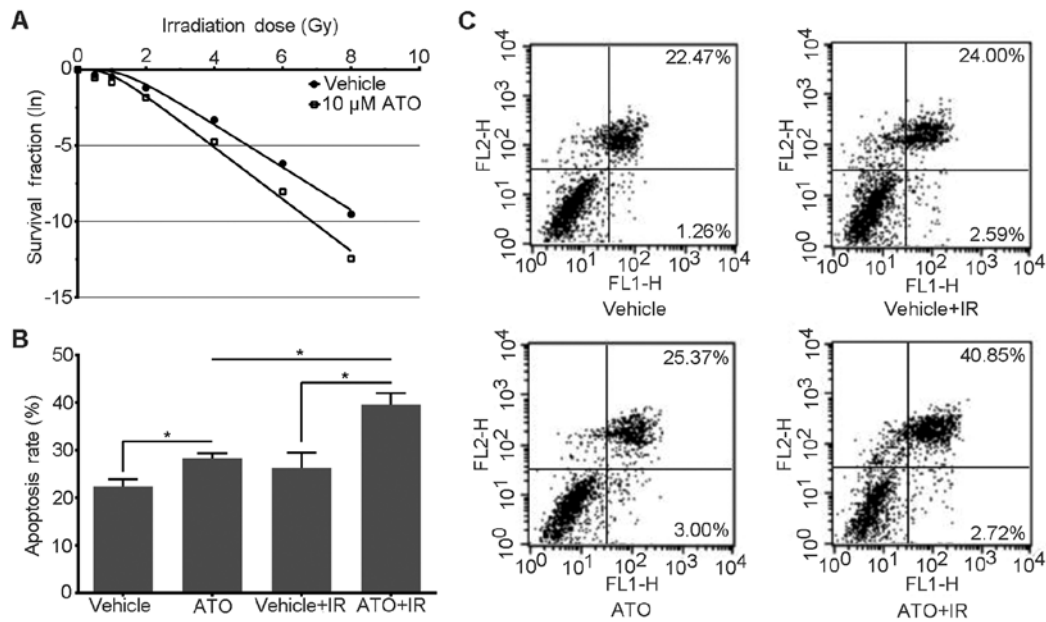
Figure 1. Analysis of the effect of ATO on the survival fraction and apoptosis rate of irradiated PC-3 cells. (A) The survival curve of PC-3 cells under different irradiation doses. Survival fractions are presented as a napierian logarithm (ln). (B) The scatterplot of flow cytometry on cell apoptosis. (C) The apoptosis rate histogram of PC-3 cells. The ATO-treated PC-3 cells received 1 Gy irradiation or were not irradiated. The data are analyzed from 4 independent experiments and expressed as the mean ± SEM, *P<0.05. ATO, atorvastatin; IR, irradiation.

temperature for 15 min. Then, the cells were incubated with Lipo3000-DNA complexes in non-serum RPMI-1640 medium, cultured in a 37˚C incubator for 6 h. Next, the old media was replaced with fresh RPMI-1640 (with 10% FBS) and cultured at 37˚C for 24 h. Finally, the transfected cells were screened using G418 antibiotic (Amresco, LLC, Solon, OH, USA) in fresh RPMI-1640 for 14 days, and the clones which were enlarged in the culture medium were selected.

ROS detection assay. PC-3 cells for flow cytometry assay were seeded into 6-well plates. Before probe treatment, the cells were collected into 15 ml tubes digested with 0.25% trypsin (with 0.05% EDTA) digestion. The cells for laser scanning confocal microscopy assay were seeded into a confocal dish. During ROS detection, part of the cells were suspended in a positive control that was diluted with non-serum RPMI-1640 medium in 1:1,000 titer and cultured in a 37˚C incubator. Fifteen minutes later, all the cells were rinsed thrice with non-serum RPMI-1640 medium, then suspended in DCFH-DA solution that was diluted with non-serum RPMI-1640 medium in 1:1,000 titer. The cells were cultured in a 37˚C incubator for 20 min and then immediately detected by flow cytometry or observed under a laser scanning confocal microscope.

For the irradiation study, the cells received a 1 Gy dose of irradiation using an Elekta linear accelerator after ATO alone or combined treatment and then the cells were cultured in a 37˚C incubator for 2 h before following the same steps as aforementioned.

Immunoblotting assay. The cells were rinsed twice with ice-cold PBS, and lysed with lysis buffer, which was supplemented with a protease inhibitor cocktail. Cell lysates were collected using a scraper and transferred into an Ependorf tube for high speed centrifugation (4˚C, 12,000 rpm, 20 min), The liquid supernatant was divided into segments of protein samples and the concentrations were determined. The protein samples were diluted with 5X loading buffer and denatured at 100˚C for 5 min.

For immunoblotting, an equal amount of total proteins from each group was separated by SDS-polyacrylamide gel electrophoresis and transferred onto PVDF membranes. Next, the antigens on the membranes were blocked with 5% dried skimmed milk/1X TBST for 1 h, and incubated overnight with corresponding primary antibodies against NOX2, NOX4, SOD1 and GAPDH, respectively. Subsequently, the membranes were washed thrice with 1X TBST and incubated with horseradish peroxidase-coupled secondary antibodies for 1 h. After washing thrice again with 1X TBST, blots on the membranes were finally detected by ECL western blotting detection reagent.

SOD activity detection. Total proteins of the PC-3 cells were extracted as aforementioned. When the protein concentration was determined, the assay was carried out according to the instructions from the total SOD assay kit with WST-8. Briefly, an equal amount of proteins was adjusted by SOD detection buffer and transferred into a 96-well plate. Then WST-8/enzyme operating solution and reaction activating solution were added. The reaction system was incubated for 30 min at 37˚C and then the absorption was detected with photometry using a microplate reader at 459 nm.

Statistical analysis. Data are expressed as the mean ± SEM. Statistic software SPSS 13.0 and GraphPad Prism 6 were used to analyze data. ImageJ software was applied to analyze the relative intensity of the protein blots. A coupled t-test was used to contrast radiosensitivity parameters and a one-way ANOVA

Table I. Parameters of the cell survival curves fitted by the multi-target single hit equation.

Parameters	n	Control	ATO group	t-stat	P-value
D_0 (Gy)	3	0.710±0.021	0.585±0.017[b]	8.013	0.001
D_q (Gy)	3	1.430±0.130	1.006±0.132[b]	3.964	0.008
N	3	7.495±1.770	5.582±1.502	1.427	0.113
SF_2	3	0.301±0.020	0.161±0.008[a]	8.774	0.013
SER_{D0}	3	1	1.277±0.065[b]	-7.381	0.001
SER_{Dq}	3	1	1.356±0.196[a]	-3.146	0.017
SER_{SF2}	3	1	1.739±0.222[b]	-5.766	0.002

Data are expressed as mean ± SEM for three independent experiments. In the ATO study group, radiosensitivity parameters (D_0, D_q, N and SF_2) were universally lower than that of the control. SERs were all >1.2. Coupled t-test displayed a statistically significant difference in parameters between the two groups (P<0.05), except N-value (P>0.05). [a]P<0.05 vs. control, [b]P<0.01 vs. control. SF_2, survival fraction at 2 Gy; SER, sensitivity enhancement ratio; ATO, atorvastatin.

was used to evaluate the apoptosis rates, ROS levels, protein levels and SOD inhibition rates. P<0.05 was defined as statistically significant; P<0.01 was considered as a highly significant difference.

Results

ATO decreases the survival fraction of irradiated PC-3 cells. To evaluate the influence of ATO on the radiosensitivity of PC-3 cells, a clonogenic assay was first conducted and a cell survival curve was plotted. As shown in the survival curve (Fig. 1A), the survival fractions of the study group were less than those of the control, especially the cells irradiated with high doses. The cell survival curves of the two groups are separated with an ampliative trend. This result implies that there was more cell killing under ATO treatment.

Using GraphPad Prism 6 fitted cell survival curve with multi-target single hit equation, the results of the radiosensitivity parameters (12) indicated that the mean values for D_0, D_q, N and SF_2 of the ATO group were universally lower than that of the control (0.585 vs. 0.710 Gy, 1.006 vs. 1,43 Gy, 5.582 vs. 7.495 Gy, 0.161 vs. 0.301 Gy, respectively). Moreover, the SERs were all >1.2 in the ATO group (Table I). A coupled t-test displayed a statistically significant difference in parameters between the two groups (P<0.05), except for the N-value (P>0.05). This indicated that ATO sensitized PC-3 cells to irradiation-mediated killing.

ATO increases the apoptosis rate of irradiated PC-3 cells. Apoptosis is the main form of cell death following irradiation (15). As the scatterplot of the flow cytometry shows (Fig. 1C), although ATO had an inducive effect on cell apoptosis in the unirradiated groups, in the irradiated groups, the apoptosis rate of the study groups was significantly increased compared with the control and late apoptosis cells were mainly predominant. The apoptosis rate in the histogram (Fig. 1B) also shows a more obvious increase in the irradiated study group compared with the control. A one-way ANOVA displayed a statistically significant difference between the two groups (P<0.05).

In addition, the apoptosis rate of the irradiated cells was significantly increased when compared with this rate in the unirradiated ATO-treated group. However, there was no statistical significance in the apoptosis rate between the irradiated and unirradiated cells in the control group.

ATO decreases the endogenetic ROS level in the PC-3 cells. To explain the radiosensitization effect of ATO, the intracellular ROS level of PC-3 cells was then detected. ROS play an important role in the cell killing process resulting from irradiation. The ROS level in cells before irradiation corresponds to the endogenetic ROS level. Our results showed that the endogenetic ROS level of the study group was obviously decreased with ATO treatment. As the result from laser scanning confocal microscopy shows (Fig. 2A), the DCF-tagged ROS fluorescence in the study group was less than that of the control. The histogram of the flow cytometry results (Fig. 2B) also shows that the ROS level of the study group dropped to nearly half the level of the negative control. A one-way ANOVA displayed a statistically significant difference between the two groups (P<0.01). These results imply that ATO decreased the endogenetic ROS level in the PC-3 cells.

However, this trend was abrogated by *NOX2* and *NOX4* gene transfection, and was exacerbated by combined treatment with tempol, which is a mimetic of SOD (Fig. 2A and B). This indicates that NOXs and SOD were responsible for the endogenetic ROS decrease.

ATO prolongs the lifespan of radiation-induced ROS. Next, the change in ROS level after irradiation was detected. Generally, radiation-induced ROS are only maintained ~10^{-9}-10^{-7} sec in cells (16,17). However, our results showed that compared with the ROS level of the control that had returned to a low level, the radiation-induced ROS of the study group was still at a high level even when the irradiation had been terminated for 2 h. The results of the laser scanning confocal microscopy showed that the DCF-tagged ROS fluorescence of the study group was more intense than that of the control (Fig. 2C). The histogram of the flow cytometry results shows that the ROS level of the study group was 4-fold more than that of the
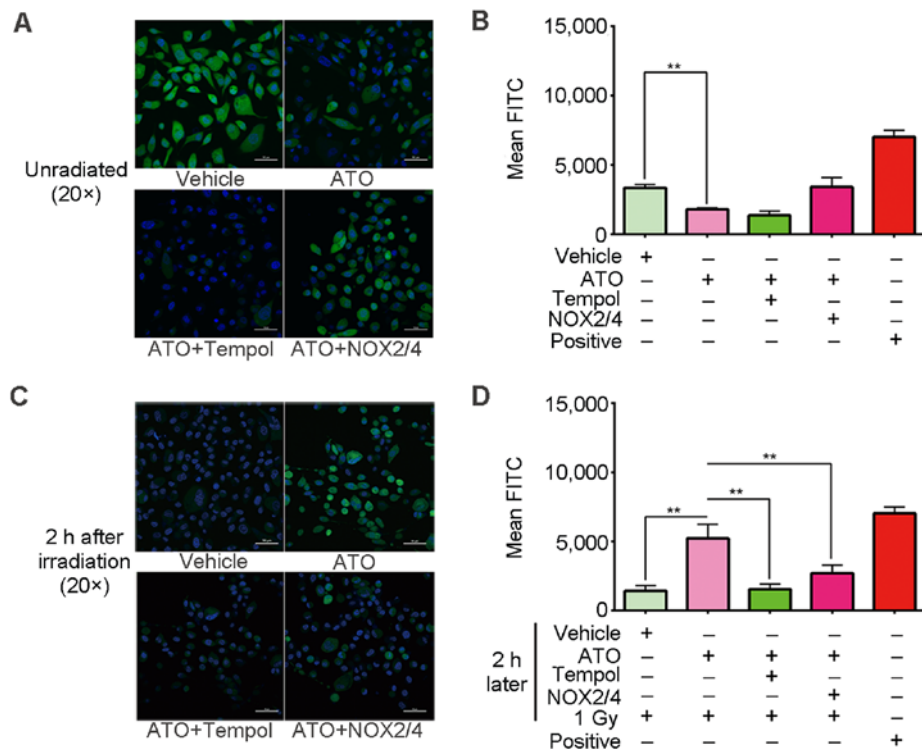
Figure 2. Effect of ATO on intracellular ROS levels. (A) Laser scanning confocal microscopy results of endogenous ROS levels. Green fluorescence indicated DCF-tagged ROS, blue fluorescence indicated nuclear staining by Hoechst. (B) Histogram of endogenous ROS levels by flow cytometry detection. (C) Laser scanning confocal microscopy results of intracellular ROS levels after the irradiation had been terminated for 2 h. (D) Histogram of intracellular ROS levels by flow cytometry detection after the irradiation had been terminated for 2 h. The data were analyzed from 3 independent experiments and are expressed as the mean ± SEM, **$P<0.01$. ATO, atorvastatin; ROS, reactive oxygen species.
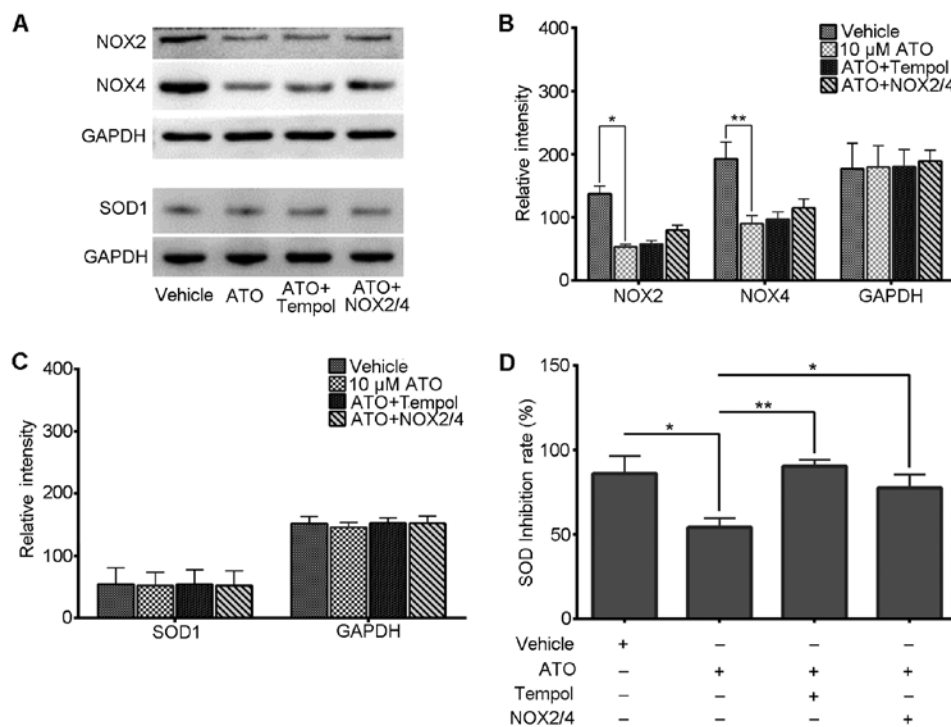

Figure 3. Effect of ATO on the levels of NOX2, NOX4 and SOD1 proteins and total SOD activity. (A) Immunoblotting results of NOX2, NOX4 and SOD1 protein levels. (B) Histogram of NOX2 and NOX4 relative expression. (C) Histogram of SOD1 relative expression. (D) Histogram of SOD inhibition rates. The data are analyzed from 3 independent experiments and are expressed as the mean ± SEM, *$P<0.05$, **$P<0.01$. ATO, atorvastatin; SOD, superoxide dismutase.

control (Fig. 2D). A one-way ANOVA displayed a statistically significant difference between the two groups ($P<0.01$). These results imply that ATO may maintain radiation-induced ROS at a lingering high level.
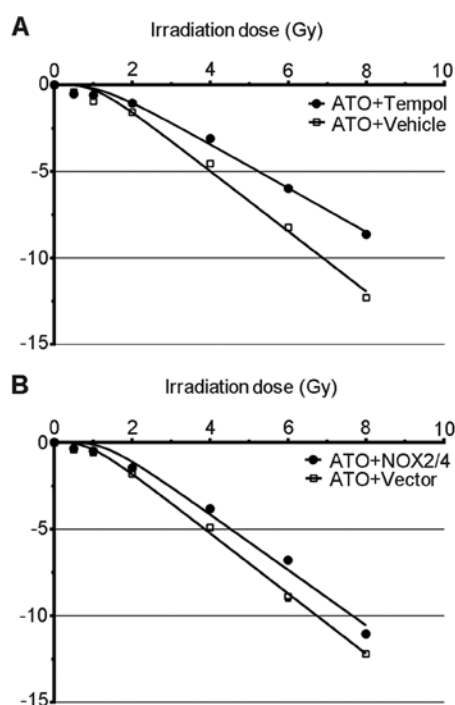
Figure 4. Changes in the survival fraction of irradiated PC-3 cells with NOX and SOD alteration. (A) The survival curve of irradiated PC-3 cells with ATO and tempol combined treatment. (B) The survival curve of irradiated PC-3 cells with combined treatment of ATO and *NOX2/4* gene transfection. ATO, atorvastatin; SOD, superoxide dismutase; NOXs, NADPH oxidases.
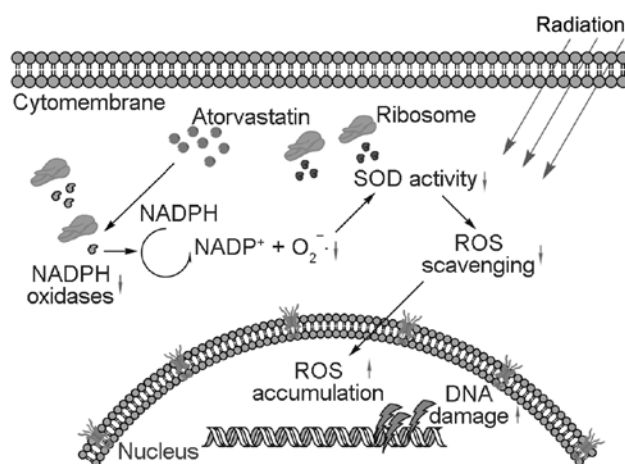

Figure 5. Model dispalying the influence of ATO on intracellular ROS and the irradiation-induced cell killing effect. i) Atorvastatin decreases endogenous ROS levels through the reduction in NOX expression, thus compensating the attenuation of SOD activity. ii) Attenuated SOD activity fails to eliminate radiation-induced ROS effectively and iii) causes accumulation of radiation-induced ROS in the cytoplasm, so that the indirect DNA damage is increased. ATO, atorvastatin; ROS, reactive oxygen species; SOD, superoxide dismutase; NOXs, NADPH oxidases.

On the other hand, the DCF-tagged ROS fluorescence of the combined treatment groups, including ATO plus tempol or *NOX* transfection, dropped to normal levels similarly to the control (Fig. 2C and D), which indicate NOXs and SOD were responsible for the high level of radiation-induced ROS as well.

ATO reduces the level of NOXs in the PC-3 cells. NOX2 and NOX4 are two isoforms that are involved in prostate cancer progression and are two main sources of endogenous ROS generation (18-20). To understand the reason for endogenetic ROS change under ATO treatment, the levels of these two protein were detected by immunoblotting. Our results showed that NOX2 and NOX4 protein blots from the study group were weaker than those noted in the control (Fig. 3A), which signifies a low expression of NOX2 and NOX4 in the study group. The histogram of relative intensity (Fig. 3B) also indicates that NOX2 and NOX4 expression levels were decreased and one-way ANOVA displayed a statistically significant difference between the two groups ($P<0.05$ and $P<0.01$). This result implies that ATO may reduce the level of NOXs in PC-3 cells.

Furthermore, our results showed that, if we transfected *NOX2* and *NOX4* genes into cells of the study group, their expression did not increase as expected, but partly increased and less than that of the levels in the control (Fig. 3A and B). On the other hand, our results also found that the addition of tempol to the study group slightly increased NOX2 and NOX4 expression, which implies that there is an association between the level of SOD and the expresssion of the NOX genes (Fig. 3A and B).

ATO reduces SOD activity in the PC-3 cells. The SOD family is able to eliminate redundant intracellular ROS in time. Based on the aforementioned results, the level of SOD was assessed. In our results, western blot analysis revealed little difference in the thickness and relative intensity of the SOD1 blots in all groups (Fig. 3A and C) and a one-way ANOVA also displayed no statistically significant difference between the groups ($P>0.05$), which suggests that the SOD1 expression underwent little change under ATO-alone treatment or the combination of treatments.

However, on the other hand, we found that the SOD activity decreased in the ATO-alone group. As our results showed (Fig. 3D), the SOD inhibition rate of the ATO-alone group decreased to nearly half of that of the control, but was restored largely when combined with tempol and was maintained at a relatively high level in the NOX transfection groups. This implies that ATO can inhibit SOD activity effectively, and this effect is related to the intracellular NOX level.

Combining ATO with tempol decreases radiosensitivity. The aforementioned results imply that a low level of endogenetic ROS and a high level of radiation-induced ROS are related to the radiosensitization effect of ATO, and a low expression of NOXs and decreased SOD activity contribute to these changes. Next, we combined ATO with *NOX* transfection or tempol to increase endogenetic ROS, or decrease radiation-induced ROS, in the clonogenic assay.

Our results indicate that combined treatment of ATO and *NOX* transfection moderately increased the survival fractions of the PC-3 cells, which had been decreased by ATO-alone treatment (Fig. 4A). On the other hand, the ATO and tempol combination greatly increased the survival fractions of the PC-3 cells compared with the ATO-alone group (Fig. 4B). These results indicate that low NOX levels and low SOD activity contribute to the sensitivity of PC-3 cells to irradiation-mediated killing.

Discussion

In the present study, we verified that ATO could increase the radiosensitivity of PC-3 cells. According to the cell survival curve, the D_0, D_q, N, and SF_2 values of the study group were all lower compared with the control. A low D_0 value implies that the mean lethal dose is lower, in other words, the dose for reducing the survival fraction from 0.1-0.037 is lower than that of the control (12), which means that PC-3 cells are prone to be killed by irradiation under ATO treatment. A low D_q and N-value imply the ability of the sublethal damage-repair to be suppressed (12), it also means that ATO-treated cells are liable to be killed by irradiation even when receiving low doses. Moreover, a low SF_2 value implies that the quantity of cells that survived that received a 2 Gy irradiation is less than that of the control (12,21). Additionally, sensitivity enhancement ratios (SERs), such as SER_{D0}, SER_{Dq} and SER_{SF2} values were all >1.2, which provides us with further evidence to conclude that ATO increases the sensitivity of PC-3 cells to radiation-induced cell killing.

Similarly, the apoptosis assay also indicated that ATO increased the apoptosis rate of the irradiated PC-3 cells. In our study, the cells that underwent ATO pretreatment and 1 Gy irradiation showed a higher apoptosis rate than the other groups, especially the cells treated with ATO alone, which implies that ATO increases radiation-induced cell killing. Apoptosis is the main form of cell death during irradiation (15). After exposure to irradiation, cells undergo either a direct effect by irradiative rays or an indirect effect by radiation-induced ROS and consequently the apoptosis process begins in tumor cells and leads to cell death. Therefore, a high apoptosis rate means more cell apoptosis under the same irradiation dose, and implies a higher radiation-induced killing effect on cells. On the other hand, a high apoptosis rate following a low dose of irradiation in cells usually implies that increased apoptosis would occur under a high dose of irradiation.

DNA damage is the key event following irradiation that causes cell death. Radiation-induced DNA damage can be defined as two types: direct damage and indirect damage. For indirect damage, its occurrence and degree are closely related to the ROS levels evoked by irradiation (22). In this respect, the more ROS generated, the more indirect damage will occur. Generally, radiation-induced ROS are only maintained for 10^{-9}-10^{-7} sec in the cell. However, our results revealed that ATO maintained radiation-induced ROS at a high level even when the irradiation was terminated for 2 h, indicating that the radiation-induced ROS levels were maintained in the cytoplasm causing persistent indirect damage to DNA. Additionally, it also implied that the ROS scavenging system, such as SOD, failed to eliminate ROS effectively.

In addition, we also found that ATO significantly decreased endogenous ROS levels in the PC-3 cells. Normally, cells may generate endogenous ROS in metabolic processes, and these play an important role in signal transduction and ensuring cell growth (23). ROS are the product of a redox reaction. A redox reaction usually maintains specific homeostasis in different types of cells (24). Normal cells maintain redox reaction homeostasis at an appropriate level and only create a moderate quantity of ROS. Conversely, tumor cells often display a hypermetabolic state so that the ROS generation is maintained

at a relatively high level (24). High ROS levels may induce high expression of ROS scavengers so as to maintain redox homeostasis. However, enhanced ROS-elimination ability allows tumor cells to endure more ROS damage, such as radiation-induced ROS and possess a radioresistant phenotype (25). Therefore, a relatively low level of endogenous ROS means a relatively high sensitivity to irradiation-induced damage and the ATO-reduced endogenous ROS level of PC-3 cells would increase its susceptibility to radiation-induced cell killing.

This effect was confirmed by adding tempol and by *NOX* tranfection. Tempol is a mimetic of SOD and the addition of tempol to culture medium enhanced the ROS-elimination ability of the PC-3 cells. Moreover, *NOX* tranfection increased ROS generation. In our results, the cells treated with ATO and tempol did not show a high level of radiation-induced ROS as aforementioned, but displayed a nearly normal level. This phenomenon confirmed that low ROS-elimination ability was the main reason for ROS accumulation. On the other hand, combining ATO with *NOX* transfection not only restored the ROS level to a normal level before irradiation, but partly weakened the high level of radiation-induced ROS as aforestated, which proves that redundant ROS that was generated by *NOX* transfection induced the ROS-elimination ability to be enhanced through a redox homeostasis mechanism.

As a crucial factor in redox reactions, NOXs are essential for endogenous ROS generation. NOX1-NOX5 are five main isoforms of the NOX family (26). In the present study, we found that ATO reduced the expression of NOX2 and NOX4, which were reported as main generators of endogenous ROS in prostate cancer (18-20). Low expression of NOX2 and NOX4 imply a reduction in endogenous ROS, and this inference complies with the result of the endogenous ROS detection aforementioned. Functionally, ATO has been reported to have antioxidant capacity in vascular endothelial cells, which is closely linked to NOXs (10). Goettsch *et al* found that ATO can inhibit NOX4 overexpression in endotheliocytes (27). Moreover, Pignatelli *et al* reported that ATO can directly inhibit the activation of NOX2 in platelets (28). Therefore, these results offer evidence to support the relationship between ATO and NOXs in PC-3 cells. In the present study, we transfected *NOX2* and *NOX4* genes into PC-3 cells and then treated these cells with ATO. However, the expression level of NOXs did not increase as expected, indicating that ATO decreased NOX2 and NOX4 expression.

The SOD family is the main scavenging system in cells for ROS elimination, especially superoxide anion ($O_2^{\bullet-}$), a main form of endogenous ROS (29). There are four SOD isoforms distributed in nature, including SOD1-SOD4 (30). SOD1 is a main isoform which is highly expressed in eukaryotic cytoplasm (31). In the present study, our findings suggested that ATO had little impact on the SOD1 level, but reduced the total SOD activity significantly. As aforementioned, redox reaction homeostasis is crucial for cell metabolism. According to our results, NOX reduction broke down previous redox homeostasis and caused a decrease in ROS. Then, the ROS scavenging system, such as SOD, was attenuated and tried to recover new homeostasis. Therefore, even when SOD1 protein levels are stably maintained, the total SOD activity attenuation still inhibits the reduction of ROS and thus can be regarded as a compensation to maintain redox homeostasis.

In contrast, a decrease in SOD activity may attenuate the ROS-eliminating capability during irradiation. Radiation-induced ROS is the product of radiolytic hydrolysis during irradiation, including superoxide anion ($O_2^{\bullet-}$), hydroxy radical ($OH^{\bullet}$) and hydrogen peroxide (H_2O_2) (32). SOD plays a pivotal role in eliminating these ROS so as to resist DNA damage. However, the decreased SOD activity fails to eliminate these ROS effectively, leading to accumulation of irradiation-induced ROS in the cells. The existence of irradiation-induced ROS accumulation aggravates the indirect DNA damage and causes more cell death.

This effect was finally verified by irradiative clonogenic assay. When we treated cells with ATO and tempol, the cell survival fraction was markedly increased compared with that of the cells treated with ATO alone, which proves that low SOD activity is responsible for the radiosensitization effect of ATO. However, when we treated cells with ATO and *NOX* transfection, the cell survival fraction also increased, but only to a level less than that of the cells treated with ATO alone, which further confirms that redundant ROS generation enhances SOD ability.

In conclusion, our data indicate that ATO is effective in decreasing endogenous ROS levels through the reduction in NOX2 and NOX4 expression and in prolonging the lifespan of irradiation-induced ROS through the attenuation of SOD activity. These effects not only increased the DNA susceptibility to irradiation, but also increased the indirect DNA damage of irradiation-induced ROS (Fig. 5) and thus enhanced the cell killing effect of irradiation in PC-3 cells.

Acknowledgements

References

1. Delaney G, Jacob S, Featherstone C and Barton M: The role of radiotherapy in cancer treatment: Estimating optimal utilization from a review of evidence-based clinical guidelines. Cancer 104: 1129-1137, 2005.
2. Seong KM, Kim CS, Jeon HY, Oh SH, Nam SY, Yang KH, Kim JY and Jin YW: Intrinsic radiosensitivity correlated with radiation-induced ROS and cell cycle regulation. Mol Cell Toxicol 6: 1-7, 2010.
3. Cooke MS, Evans MD, Dizdaroglu M and Lunec J: Oxidative DNA damage: Mechanisms, mutation, and disease. FASEB J 17: 1195-1214, 2003.
4. Goldstein JL and Brown MS: Regulation of the mevalonate pathway. Nature 343: 425-430, 1990.
5. Park HS, Schoenfeld JD, Mailhot RB, Shive M, Hartman RI, Ogembo R and Mucci LA: Statins and prostate cancer recurrence following radical prostatectomy or radiotherapy: A systematic review and meta-analysis. Ann Oncol 24: 1427-1434, 2013.
6. He Z, Mangala LS, Theriot CA, Rohde LH, Wu H and Zhang Y: Cell killing and radiosensitizing effects of atorvastatin in PC3 prostate cancer cells. J Radiat Res (Tokyo) 53: 225-233, 2012.
7. Fritz G, Brachetti C and Kaina B: Lovastatin causes sensitization of HeLa cells to ionizing radiation-induced apoptosis by the abrogation of G2 blockage. Int J Radiat Biol 79: 601-610, 2003.
8. Mihăilă RG: Advances in the management of malignant hemopathies: The role of statins. Recent Pat DNA Gene Seq 7: 57-61, 2013.
9. Song X, Liu BC, Lu XY, Yang LL, Zhai YJ, Eaton AF, Thai TL, Eaton DC, Ma HP and Shen BZ: Lovastatin inhibits human B lymphoma cell proliferation by reducing intracellular ROS and TRPC6 expression. Biochim Biophys Acta 1843: 894-901, 2014.
10. Wassmann S, Laufs U, Müller K, Konkol C, Ahlbory K, Bäumer AT, Linz W, Böhm M and Nickenig G: Cellular antioxidant effects of atorvastatin in vitro and in vivo. Arterioscler Thromb Vasc Biol 22: 300-305, 2002.
11. Leith JT, Quaranto L, Padfield G, Michelson S and Hercbergs A: Radiobiological studies of PC-3 and DU-145 human prostate cancer cells: X-ray sensitivity *in vitro* and hypoxic fractions of xenografted tumors in vivo. Int J Radiat Oncol Biol Phys 25: 283-287, 1993.
12. Tucker SL: Parameters of radiosensitivity. Radiat Res 108: 226-229, 1986.
13. Oliver R and Shepstone B: Some practical considerations in determining the parameters for multi-target and multi-hit survival curves. Phys Med Biol 9: 167-175, 1964.
14. Jones KJ, Chetram MA, Bethea DA, Bryant LK, Odero-Marah V and Hinton CV: Cysteine (C)-X-C receptor 4 regulates NADPH oxidase-2 during oxidative stress in prostate cancer cells. Cancer Microenviron 6: 277-288, 2013.
15. Verheij M and Bartelink H: Radiation-induced apoptosis. Cell Tissue Res 301: 133-142, 2000.
16. Kim GJ, Fiskum GM and Morgan WF: A role for mitochondrial dysfunction in perpetuating radiation-induced genomic instability. Cancer Res 66: 10377-10383, 2006.
17. Lesser MP: Oxidative stress in marine environments: Biochemistry and physiological ecology. Annu Rev Physiol 68: 253-278, 2006.
18. Kumar B, Koul S, Khandrika L, Meacham RB and Koul HK: Oxidative stress is inherent in prostate cancer cells and is required for aggressive phenotype. Cancer Res 68: 1777-1785, 2008.
19. Lu JP, Hou ZF, Duivenvoorden WC, Whelan K, Honig A and Pinthus JH: Adiponectin inhibits oxidative stress in human prostate carcinoma cells. Prostate Cancer Prostatic Dis 15: 28-35, 2012.
20. Lu JP, Monardo L, Bryskin I, Hou ZF, Trachtenberg J, Wilson BC and Pinthus JH: Androgens induce oxidative stress and radiation resistance in prostate cancer cells though NADPH oxidase. Prostate Cancer Prostatic Dis 13: 39-46, 2010.
21. Deacon J, Peckham MJ and Steel GG: The radioresponsiveness of human tumours and the initial slope of the cell survival curve. Radiother Oncol 2: 317-323, 1984.
22. Kryston TB, Georgiev AB, Pissis P and Georgakilas AG: Role of oxidative stress and DNA damage in human carcinogenesis. Mutat Res 711: 193-201, 2011.
23. Boonstra J and Post JA: Molecular events associated with reactive oxygen species and cell cycle progression in mammalian cells. Gene 337: 1-13, 2004.
24. Zhang Y and Martin SG: Redox proteins and radiotherapy. Clin Oncol (R Coll Radiol) 26: 289-300, 2014.
25. Trachootham D, Alexandre J and Huang P: Targeting cancer cells by ROS-mediated mechanisms: A radical therapeutic approach? Nat Rev Drug Discov 8: 579-591, 2009.
26. Lambeth JD: NOX enzymes and the biology of reactive oxygen. Nat Rev Immunol 4: 181-189, 2004.
27. Goettsch C, Goettsch W, Muller G, Seebach J, Schnittler HJ and Morawietz H: Nox4 overexpression activates reactive oxygen species and p38 MAPK in human endothelial cells. Biochem Biophys Res Commun 380: 355-360, 2009.
28. Pignatelli P, Carnevale R, Pastori D, Cangemi R, Napoleone L, Bartimoccia S, Nocella C, Basili S and Violi F: Immediate antioxidant and antiplatelet effect of atorvastatin via inhibition of Nox2. Circulation 126: 92-103, 2012.
29. Nathan C and Cunningham-Bussel A: Beyond oxidative stress: An immunologist's guide to reactive oxygen species. Nat Rev Immunol 13: 349-361, 2013.
30. Youn HD, Kim EJ, Roe JH, Hah YC and Kang SO: A novel nickel-containing superoxide dismutase from *Streptomyces* spp. Biochem J 318: 889-896, 1996.
31. Juarez JC, Manuia M, Burnett ME, Betancourt O, Boivin B, Shaw DE, Tonks NK, Mazar AP and Doñate F: Superoxide dismutase 1 (SOD1) is essential for H_2O_2-mediated oxidation and inactivation of phosphatases in growth factor signaling. Proc Natl Acad Sci USA 105: 7147-7152, 2008.
32. Riley PA: Free radicals in biology: Oxidative stress and the effects of ionizing radiation. Int J Radiat Biol 65: 27-33, 1994.